RESEARCH ARTICLE

Optimizing Fault Ride-Through of DGs in Distribution Networks to Preserve Recloser-Fuse Coordination

EVANGELOS E. POMPODAKIS[iD]**, YIANNIS A. KATSIGIANNIS,**
AND EMMANOUEL S. KARAPIDAKIS[iD]

Department of Electrical and Computer Engineering, Hellenic Mediterranean University, 731 33 Chania, Greece

Corresponding author: Evangelos E. Pompodakis (bobodakis@hotmail.com)

ABSTRACT Fuse saving protection is usually applied in distribution networks, through auto-reclosing, to prevent fuse burning under transient faults. The modern fault ride-through (FRT) standards, which require distributed generators (DGs) to remain connected during the fault, may lead to the miscoordination of recloser-fuse. This paper proposes a discrete coordinate-descent (DCD) approach that optimizes the FRT of DGs so that the coordination between recloser and fuse is preserved. First, the method performs a short-circuit calculation (SCC) considering the currents contributed by the DGs, according to the FRT standards of each country. Then, if a miscoordination between recloser-fuses is observed, it optimally scales down the DG currents, until the coordination is restored. The proposed method has simple implementation, low communication requirements and offers adequate voltage support during the fault. Simulations were carried out in the IEEE 13-bus and the IEEE 8500-node network to highlight the distinct features of the proposed approach against the state-of-the-art current limiting approaches.

INDEX TERMS Discrete coordinate descent, distribution networks, fault ride-through, fuse, optimization, protective device coordination, recloser, short-circuit.

NOMENCLATURE

Subscripts	Description	Unit
dg	Number of DGs	-
Iter	Total iteration numbers of the DCD algorithm	-
t	Iteration number of DCD algorithm	-
sl	Slow recloser curve	-
fa	Fast recloser curve	-
h.i.	High-impedance (5 Ohm) fault	-
l.i.	Low-impedance (0 Ohm) fault	-
f1	Fuse 1	-
RC 1	Recloser 1	-
l.i. f1	0-Ohm fault at the beginning of the lateral protected via f1	-
h.i. f1	5-Ohm fault at the end of the lateral protected via f1	-
H(•)	Heaviside function	-
min(x, y)	Outputs the minimum between x and y	

VARIABLES

$T_{f,hi}^t$	Tripping time of fuse for a high impedance fault downstream the fuse	s
$T_{f,li}^t$	Tripping time of fuse for a low impedance fault downstream the fuse	s
$T_{rc,sl \to f,hi}^t$	Tripping time of the slow recloser for a high impedance fault downstream the fuse f	s

The associate editor coordinating the review of this manuscript and approving it for publication was Arturo Conde[iD].

$T^t_{rc,fa \rightarrow f,li}$	Tripping time of the fast recloser for a low impedance fault downstream the fuse f	s
$T^t_{rc,fa \rightarrow f,hi}$	Tripping time of the fast recloser for a high impedance fault downstream the fuse f	s
$I^t_{f,hi}$	Fault current through the fuse for a high impedance fault downstream the fuse	s
$I^t_{f,li}$	Fault current through the fuse for a low impedance fault downstream the fuse	s
$I^t_{rc \rightarrow f,hi}$	Fault current through the recloser for a high impendence fault downstream the fuse	s
$I^t_{rc \rightarrow f,li}$	Fault current through the recloser for a low impendence fault downstream the fuse	s
K^t_i	Fault current limiter of DG i at iteration t	-
dK	Variation step of fault current limiter in the DCD algorithm	-
$P_{(i)}$	Active power of DG i	W
$I_{max(i)}$	Maximum current of DG i (restricted by its semiconductors)	A
$I^t_{gen(i)}$	Fault current injected by DG i at iteration t (after the limitation)	A
$I_{FRT(i)}$	Current injected by DG i, according to the FRT standard (before the limitation)	A
$V_{(i)}$	Positive-sequence voltage of DG i	V
V_{nom}	Nominal Voltage	V
$R_{pcc(i)}$	Per unit voltage of DG i,e.g., $R_{pcc(i)} = V_{(i)}/V_{nom}$	pu
Z_f	Fault impedance	Ω

I. INTRODUCTION

A. MOTIVATION AND CHALLENGES

Fuse saving schemes consist of a recloser located at the head of the feeder and fuse(s) located at the laterals, downstream the recloser [1]. They are usually applied in distribution networks to prevent the fuse burning in case of transient faults, avoiding the additional cost of replacing fuses and reducing the lateral outage time [2]. The modern FRT standards require DGs to remain connected during the fault [3], which may lead to the miscoordination of recloser-fuse, degrading the selectivity and reliability indices [4], [5]. Specifically, the current generated by DGs, during the fault, may modify differently the fault current sensed by the recloser and fuse respectively, affecting unequally their tripping times. Several solutions to the problem have been proposed in the literature, which can be divided into night (10) categories:

- DG disconnection: DGs are immediately disconnected as soon as they sense the fault [6].Although this strategy does not disrupt the coordination of protective devices (PD),

it causes massive renewable outages even under transient faults, resulting in frequent voltage dips and renewable power loss.

- Limit DG penetration: DGs are connected only to appropriate locations and up to a maximum level, where the PD coordination is not disrupted [7], [8], [9]. Despite its simplicity, this method is not a desired option since it clearly restricts the penetration of DGs and does not comply with the decarbonization goal of the electricity sector.

- Fault current limiters (FCL): Fault current limiters are physical devices, which have a low impedance under normal conditions, while they rapidly increase it as soon as a high current is flown through them [10], [11]. When they are suitably located in series with the DGs, they restrict their fault current, preventing the malfunction of the PDs. However, they cause high losses in normal operation; they have long recovery time and increased cost.

- Replacement/Resizing of protective devices: To prevent miscoordination among protective devices in the presence of DGs, recloser settings are adjusted, while fuses are resized according to the scenario with the highest DG current injection [12]. However, resizing protective devices based on the highest DG penetration level addresses misoperations only during peak penetration periods, potentially compromising sensitivity during periods of low DG penetration.

- Adaptive (online) protection schemes: The settings of recloser are adapted, in real-time, depending on the current and location of DGs so that the coordination of PDs is preserved [3], [4], [13], [14], [15], [16], [17]. These schemes require microprocessor-based reclosers and an extensive communication infrastructure between the recloser and the distribution control center (DCC), which is not always available [18]. Moreover, fuses have fixed (non-adaptable) characteristics, restricting the flexibility of adaptive protection schemes. For instance, if large DGs are located upstream of the fuse, they have the potential to cause the fuse to burn out faster than the minimum recloser time allows.

- Energy storage systems (ESS): ESSs have been presented as a promising solution for coordinating PDs. They can provide a sufficient fault current in networks with low short circuit capacity such as islanded microgrids [19], [20], substituting the high current of substation. Nevertheless, ESSs do not sufficiently solve the problem of miscoordination between recloser-fuses; instead, like DGs, they may burden it due to the additional current they provide. Moreover, ESSs constitute a costly solution and are not recommended for addressing protection issues.

- Differential/distance protection: Distance relays are the traditional PDs for transmission networks. They estimate the distance to the fault, considering the relative position of DGs [21], and they are tripped if the distance is within their protection zone. However, the distance estimation is not always accurate since it is affected by the time-varying current of DGs; furthermore, it is a costly solution for applications in distribution networks. Differential relays can isolate the faulty feeder regardless of the current of DGs [22], [23].

However, it is not a cost-effective solution since it requires fast communication links between the two ends of relays.

- Multiagent-based methods: In such instances, fault clearance relies on information exchanged among system components acting as agents, including DGs, PDs, and current transformers [2]. However, these methods require fast communication for transferring real-time data between agents, and their performance is sacrificed in case of communication failures or delays. Moreover, they are unsuitable for systems with a substantial number of PDs due to the expenses associated with modifications, which could potentially outweigh the economic advantages of DGs.

- DG current limiters: The current of DGs is properly controlled (limited or shifted), during the fault, to support the voltage, while at the same time, the PD coordination is preserved [18], [24], [25], [26], [27], [28], [29], [30], [31], [32]. Since the scope of this paper is to propose a DG current limiting approach, a literature review of only this category is provided below.

B. LITERATURE REVIEW ON DG CURRENT LIMITERS

In [24], the current magnitude of DGs is set to a pre-specified value determined by offline analysis to ensure that the PD coordination is not disrupted. However, this approach is very pessimistic since it takes the worst-case scenario, and thus it does not fully utilize the capability of DGs to support the voltage during the fault.

In [25], the influence of DGs on the protection equipment is prevented by controlling the phase angle of DG current, during the fault, instead of the magnitude. However, when many DGs are installed, the phasor relation between the fault current elements becomes increasingly complex, and the desired current phase angles of DGs are not easily computed [25, p. 2118]. In [26], a new reference current calculation algorithm is developed in the *abc* frame involving the phase angle shifting of DG current on faulted phase, achieving power ripple elimination. In [27], a hierarchical approach is proposed for controlling the DG fault current. Initially, the DG fault current is calculated considering the German FRT code, and subsequently, the phase angle is shifted to neutralize its effect on the PDs. In [28], the fault current of multiple DGs is optimized using interior point optimization, to maintain the operating times of individual PDs within a narrow band after IBDGs integration. Although the approaches of [25], [26], [27], and [28] preserve the PD coordination and enforce DGs to provide current supporting the voltage during the fault, they require advanced metering and fast communication infrastructure to locate the fault and assign DGs with optimal real-time settings. Moreover, they are sensitive to measurement and communication errors or delays.

A decentralized method for limiting DG current during the fault is proposed in [29]. Specifically, the DG current is reduced depending on its terminal voltage. The idea is that DGs located near the fault are more possible to cause miscoordination of PDs, and thus, they are imposed a higher current

limitation (see [29, eq. (10)]). The same limiting factor on the DG current is applied in [30] as well. In [31], authors improved the method of [29], by measuring the line current, instead of only the DG voltage, to avoid unnecessary current reductions in high impedance faults or temporary voltage dips. However, the method of [31] requires advanced sensor and communication infrastructure between the fuse and the DGs, which is not always available. A decentralized current limiter of DG current is adopted in [18, eq. (5)] and [32, eq. (17)] as well. Although the methods in [18], [29], [30], [31], and [32] do not need any advanced metering and communication infrastructure, they fail to preserve recloser-fuse coordination under certain circumstances. Moreover, they usually reduce the DG current non-optimally, to a too small magnitude, even in situations where such reduction is unnecessary, deteriorating the voltage support of the network. More details about the drawbacks of [18], [29], [30], [31], and [32] are provided in sections II, IV and V.

C. CONTRIBUTION OF THE PAPER

To overcome the drawbacks of the cited references, this paper presents a DG fault current limiting approach with low communication and metering requirements. The method first calculates DG fault currents as mandated by the FRT standards. If a miscoordination between recloser-fuses is observed, it optimally scales down the current, using DCD optimization, until the PD coordination is restored.

The proposed optimization approach has the following distinct features:

- It has simple implementation since it requires only a conventional short-circuit solver such as [33] and [34], without the need of optimization software, e.g., GAMS etc.
- Unlike [25], [26], [27], [28], which necessitate real-time data transmission from smart meters to DGs during the fault, our proposed approach doesn't demand high data rate; instead, only low-bandwidth communication channels between the DCC and DGs are required, which are commonly available in modern distribution networks [35]. Specifically, the method simply sends optimal current limiting factors to DGs, either periodically, e.g., every hour, or upon request after a network reconfiguration.
- The optimization is based on the practically accepted DCD algorithm, which is state-of-the-art in real-time distribution management system (DMS) applications, e.g., Volt-Var control [36], [37]; thus, it can be easily incorporated in existing DMS, as an additional function, for optimizing the FRT of DGs to preserve the PD coordination.
- It offers a better voltage support in most low-impedance faults than the decentralized current limiting methods of [18], [29], [30], [31], and [32].
- In contrast to the decentralized methods, the proposed approach always ensures PD coordination.

II. RECLOSER-FUSE MISCOORDINATION

A. MODERN FAULT-RIDE THROUGH STANDARDS

The ever-growing penetration of distributed generators has led many countries to revise their FRT standards by imposing DGs not to be disconnected immediately after the fault, but remain connected for a specified period, injecting balanced reactive current[1] [38], [39], [40]. The injected current and the time that DGs remain connected depend on the positive-sequence voltage of DGs [38], [39], [40]. Specifically, for the German code, the injected positive-sequence reactive current and disconnection time of DGs is depicted in Fig. 1a and 1b, respectively, as a function of the per unit positive-sequence voltage [38], [40]. As shown, the disconnection time of DGs is linearly dependent on the terminal voltage of DGs. Moreover, there is a minimum time of 150 ms that DGs should remain connected regardless the severity of the fault.

The reactive $\left(I_{q(i)}\right)$ and active $\left(I_{d(i)}\right)$ current components of DG i are calculated by (1a)-(1b), while the FRT current of DG by (1c). All the variables have been defined in nomenclature.

$$I_{q(i)} = \min\left(2 \cdot I_{max(i)} \cdot \left(1 - R_{pcc(i)}\right), I_{max(i)}\right) \quad (1a)$$

$$I_{d(i)} = \min\left(\frac{P_{(i)}}{3 \cdot V_{(i)}}, \sqrt{I_{max(i)}^2 - I_{q(i)}^2}\right) \quad (1b)$$

$$I_{FRT(i)} = I_{d(i)} + I_{q(i)} \cdot j \quad (1c)$$

B. PROTECTION SYSTEM MISCOORDINATION

In this section, the miscoordination of recloser-fuse due to the connection of DGs is analyzed, using the example network of Fig. 2, protected through a RC-fuse pair. The time-current curves of the RC-fuse are shown in Fig. 3. Recloser has two curves: The fast one forces the recloser to open before the fuse to prevent the burning of the fuse, in case of a transient fault. The recloser remains open for a short period (around 0.5s) to extinguish the transient fault, and then closes again. If the fault persists after reclosing, the fuse blows out. The slow curve of the recloser operates as a backup protection in case the fuse fails.

In the absence of DGs, recloser and fuse carry almost the same current (a small difference exists due to the loads). The coordination interval of recloser-fuse is shown in Fig. 3, where I_{f-min} corresponds to the lowest fault current (highest fault impedance) taking place downstream the fuse, while I_{f-max} to the highest (lowest fault impedance). For faults within this interval, coordination is achieved; the tripping order is *fast recloser→fuse→slow recloser*. A coordination time interval (CTI) of 50 ms is usually taken between the curves as a safety margin. Note that for the sake of clarity, the CTI has been ignored in this paper (namely CTI=0), although it can be easily incorporated in the proposed approach, if desired.

---

[1]Some countries have revised their FRT codes by imposing DGs to inject also negative-sequence active and reactive current [41]. Due to space limitation, this case is not examined here.
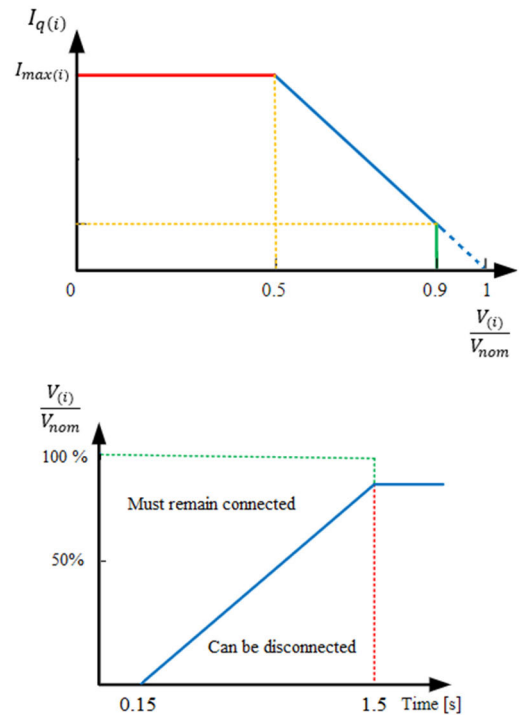
FIGURE 1. German FRT code [38], [40]. From top to bottom: a) required reactive current injection, b) time required for DG to remain connected after the fault.
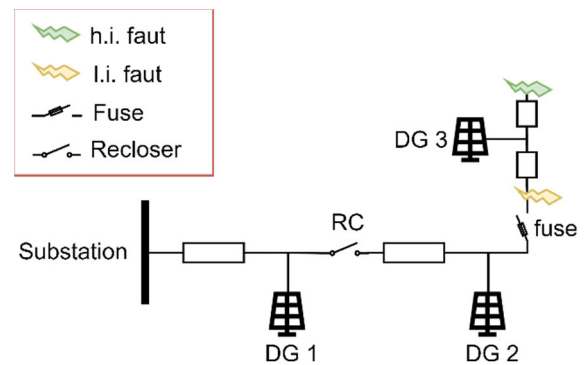

FIGURE 2. Example network consisting of a recloser-fuse pair, and 3 DGs located at different locations.

The influence of DGs on the recloser-fuse coordination is highlighted by connecting three DGs as shown Fig. 2. As shown, DG 1 is upward the recloser, DG 2 is between the pair, while DG 3 is downward the fuse. DGs affect in a completely different way the coordination causing 4 different types of miscoordination. Note that the following classification is given in this paper only for the sake of clarity, and it is not a standardized classification.

- *Type 1 miscoordination*: DG 1 shifts all the curves to the right, as shown in Fig. 4, jeopardizing the coordination between the fuse and fast RC in low impedance (l.i.) faults.
- *Type 2 & 3 miscoordination*: DG 2 shifts the curves of RC to the left and fuse to the right, as shown in Fig. 5,
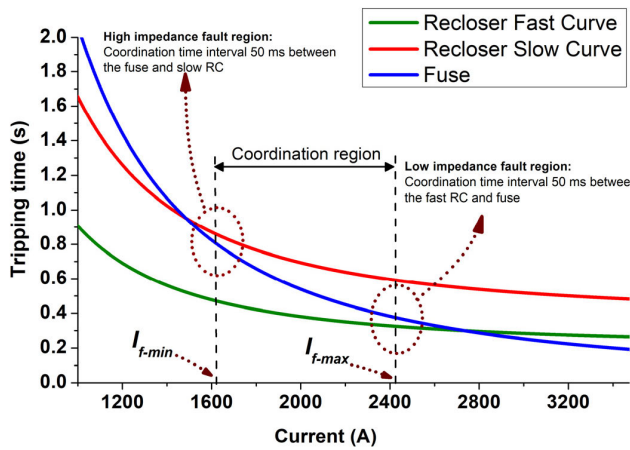
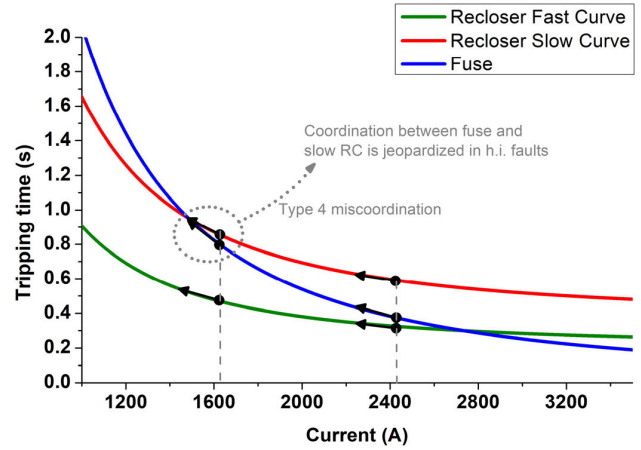**FIGURE 3.** Time-current curves and coordination region of recloser-fuse, without the DGs.

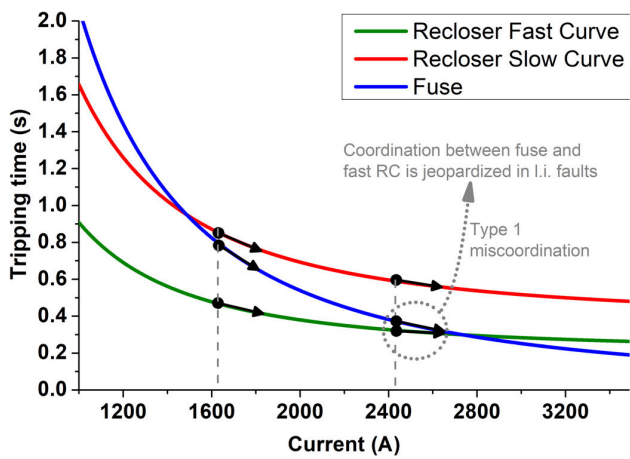**FIGURE 4.** Type 1 miscoordination due to DG 1.

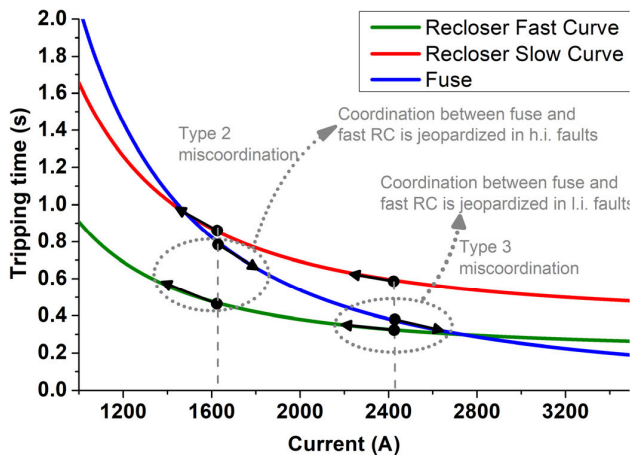**FIGURE 5.** Type 2 and type 3 miscoordination due to DG 2.

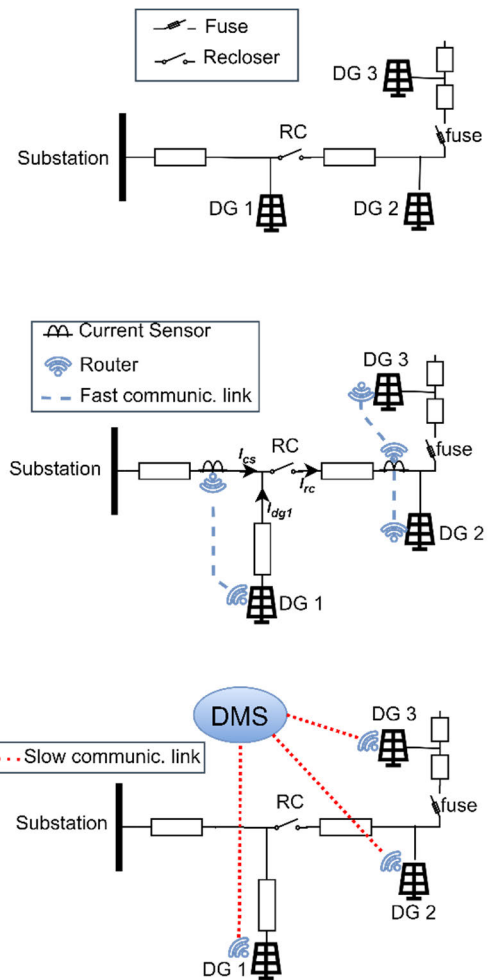**FIGURE 6.** Type 4 miscoordination due to DG 3.

FIGURE 7. From top to bottom: Communication structure of a) decentralized current control [18], [29], [30], [31], [32], b) real-time measurement-based control [25], [26], [27], [28], c) proposed DMS-based approach.

jeopardizing the coordination between the fuse and fast RC in both high impedance (h.i.) and l.i. faults.

- *Type 4 miscoordination*: DG 3 shifts all the curves to the left, as shown in Fig. 6, jeopardizing the coordination between the fuse and slow RC in h.i. faults.

C. PREVENTING MISCOORDINATION VIA DG CONTROL

For restoring the recloser-fuse coordination via DG current control, two fundamental approaches have been presented in the literature, which are depicted in Figs. 7a and 7b:

the decentralized and the real-time measurement-based approaches. The decentralized methods (Fig. 7a) do not require any communication infrastructure. DGs limit their current in proportion to their voltage drop. Nevertheless, under circumstances, decentralized methods may fail to prevent miscoordination, as proved in sections IV-V.

The communication structure of the real-time measurement-based current limiting methods [25], [26], [27], [28] is quoted in Fig. 7b. As shown, current sensors need to be strategically placed within the network to transmit (in real time) their measurements to DGs. DGs do not alter the magnitude of their current; instead, they adjust the phase angle, such that the magnitude of the current flowing through the PDs remains consistent with the pre-DG connection state. For instance, looking at Fig. 7b, if a fault occurs downstream of the fuse, the first current sensor transmits its current measurement to DG 1. DG 1 does not reduce its current; instead, it adjusts its phase, until the current magnitude flowing through the sensor $\left(\left|\vec{I}_{cs}\right|\right)$ and recloser $\left(\left|\vec{I}_{rc}\right|\right)$ become equal, e.g., $\left|\vec{I}_{cs}\right| = \left|\vec{I}_{rc}\right|$. Similarly for the other DGs. In this way, the coordination is not disrupted since all PDs sense the same current as before the connection of DGs, while DGs provide fault current supporting the network voltage. However, the requirement for extensive communication and measurement infrastructure is an issue for this approach. Moreover, the efficiency of these schemes may be significantly affected by measurement and communication errors and/or delays.

The graph of the proposed current limiting method is shown in Fig. 7c. It is incorporated as an additional application in the DMS to optimize the current limiting factors (CLF) of DGs. If a fault occurs, DGs do not inject their full FRT currents, but limit them by optimized CLFs (note that CLF≤1). The proposed approach does not require fast communication equipment since it transmits the optimal CLFs to DGs either periodically, e.g., every hour, or upon request after a topology change; thus, DGs respond to the fault in a decentralized manner. This reduction in data rate enhances resilience against communication failures. For example, short communication interruptions, such as those lasting below 1 hour, have no impact on our proposed approach. This stands in stark contrast to the approaches in [25], [26], [27], and [28], where similar disruptions would significantly hinder performance. Moreover, the proposed approach complies with the FRT code of each country since it only slightly limits the current, up to the point that the coordination is not disrupted. Finally, it is shown in the simulations that it usually provides a better voltage support than the decentralized methods [18], [29], [30], [31], [32], while always ensures coordination.

III. DISCRETE COORDINATE DESCENT ALGORITHM
A. BACKGROUND
The DCD optimization algorithm is an industry standard for practical DMS applications such as Volt-Var control (VVC) [36], [37]. The algorithm is called coordinate-descent because only one coordinate (control variable) is optimized

at each iteration, and discrete because the coordinate update is taken in a discrete step [36], [42]. The most important versions of DCD are the randomized coordinate descent (RCD) and greedy coordinate-descent (GCD) [42], [43] etc. RCD randomly selects a coordinate to update at each iteration, while GCD selects the coordinate that makes the most progress [43]. In this paper, we used the greedy DCD algorithm. Specifically, each iteration requires computing the objective function for each possible search direction of every control variable; in our problem, control variable is the CLF of each DG and search direction is a discrete reduction. The control variable that gives the greatest decrease in objective function is selected to move to the optimal search direction [36]. The algorithm is executed until there is no search direction giving an improvement in the objective function.

The scope of our application is to optimally restrict the DG currents until the coordination between all the recloser-fuse pairs is restored. Fig. 3 depicts the time-current curves of a recloser-fuse pair, which can be divided into three regions: a) high fault impedance region, b) medium fault impedance region, c) low fault impedance region ($Z_f < 0.1\Omega$). In the medium fault impedance region, the coordination between recloser-fuse is not threatened, even under a large DG penetration, since there is sufficient margin between the fuse and the recloser curves. On the other hand, in the high and low impedance regions, the coordination may be disrupted because of the DGs. The idea is that if the coordination is ensured at the low and high impedance regions, it is also ensured for all the range of fault impedances. For this reason, in the mathematical formulation below, we ignore the medium impedance region, considering only the 4 types of miscoordination explained in section II-B, at the low and high impedance regions.

B. MATHEMATICAL FORMULATION
The mathematical formulation of the proposed DCD optimization approach is presented here. For clarity, the network of Fig. 2 is used to formulate the equations. However, the proposed approach is flexible and can be expanded in large networks with many recloser-fuse pairs, by just adding in the cost function (2), the corresponding miscoordination costs of all recloser-fuse pairs (see Appendix for expansion). The objective (cost) function is given in (2).

$$f = \overbrace{\left(T_{f,hi}^t - T_{rc,sl \to f,hi}^t\right)^2 \cdot \mathrm{H}\left(T_{f,hi}^t - T_{rc,sl \to f,hi}^t\right)}^{\text{Type 4 miscoordination}}$$

$$+ \underbrace{\left(T_{rc,fa \to f,hi}^t - T_{f,hi}^t\right)^2 \cdot \mathrm{H}\left(T_{rc,fa \to f,hi}^t - T_{f,hi}^t\right)}_{\text{Type 2 miscoordination}}$$

$$+ \overbrace{\left(T_{rc,fa \to f,li}^t - T_{f,li}^t\right)^2 \cdot \mathrm{H}\left(T_{rc,fa \to f,li}^t - T_{f,li}^t\right)}^{\text{Type 1 \& 3 miscoordination}} \quad (2)$$

All variables in (2) are defined in the nomenclature and calculated in (3)-(7). Specifically, equation (3) is derived by
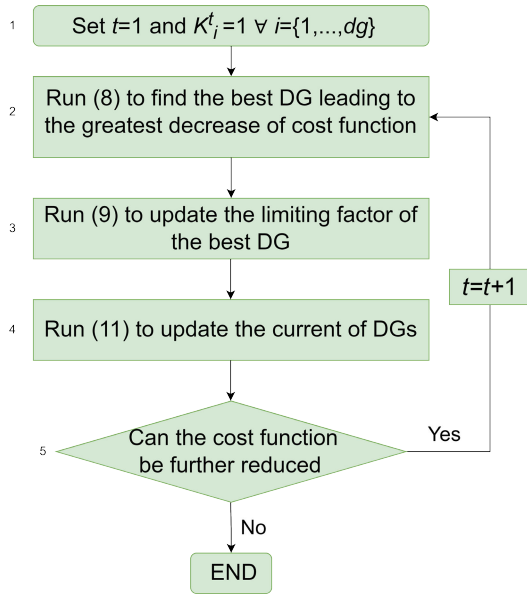
FIGURE 8. Flowchart of the proposed DCD optimization approach.

[1, eq. (2)] and calculates (at iteration t) the tripping time of the fuse ($T^t_{f,hi}$), as a function of its current ($I^t_{f,hi}$), for a high impedance fault, while (4) for a low impedance fault.

$$T^t_{f,hi} = 10^{(\alpha \cdot log_{10}(I^t_{f,hi})+b)} \forall t \in \{1, \dots, Iter\} \qquad (3)$$

$$T^t_{f,li} = 10^{(\alpha \cdot log_{10}(I^t_{f,li})+b)} \forall t \in \{1, \dots, Iter\} \qquad (4)$$

Equation (5) calculates the tripping time of the slow recloser curve at iteration $t(T^t_{rc,sl \to f,hi})$, as a function of its current ($I^t_{rc \to f,hi}$), for a high impedance fault downstream of the fuse [16, eq. (3)]. Equations (6) and (7) calculate the same for the fast recloser under a low and high impedance fault, respectively.

$$T^t_{rc,sl \to f,hi} = TDS \cdot \left(\frac{B}{\left(\frac{I^t_{rc \to f,hi}}{I_p}\right)^a - 1} + C \right)$$
$$\forall t \in \{1, \dots, Iter\} \qquad (5)$$

$$T^t_{rc,fa \to f,li} = TDS \cdot \left(\frac{B}{\left(\frac{I^t_{rc \to f,li}}{I_p}\right)^a - 1} + C \right)$$
$$\forall t \in \{1, \dots, Iter\} \qquad (6)$$

$$T^t_{rc,fa \to f,hi} = TDS \cdot \left(\frac{B}{\left(\frac{I^t_{rc \to f,hi}}{I_p}\right)^a - 1} + C \right)$$
$$\forall t \in \{1, \dots, Iter\} \qquad (7)$$

The objective function (2) quantifies the miscoordination cost between the recloser-fuse, for all types of miscoordination, classified in section II-B. For example, the first term of

the objective function, e.g., $\left(T^t_{f,hi} - T^t_{rc,sl \to f,hi}\right)^2$, quantifies the cost of "*type 4 miscoordination*". The Heaviside function (H) is used to nullify the cost if the coordination is restored, e.g., $T^t_{f,hi} < T^t_{rc,sl \to f,hi}$.

Equation (8) finds the argument of the maximum of the gradient of cost function f. Specifically, it finds at each iteration t the optimal DG d that leads, via the reduction of its current limiting factor (K^t_d), to the greatest reduction of the objective function (2). Namely, it finds the DG d with the maximum $\frac{\partial f}{\partial K^t_d}$ gradient (f is the objective function).

$$d \in \underset{j=\{1,\dots,dg\}}{argmax} \left| \nabla_j f \left(K^t_1, \dots, K^t_{dg}\right) \right| \forall t \in \{1, \dots, Iter\} \quad (8)$$

The current limiting factor of the (best) DG d is reduced in (9), by a pre-specified step dK, provided that it lies within the minimum (0) and maximum (1) limit, according to (10). The step dK is arbitrarily selected. High values of dK result in a faster convergence of the DCD algorithm but with a lower accuracy.

$$K^{t+1}_d = K^t_d - dK \ \forall t \in \{1, \dots, Iter\} \qquad (9)$$
$$0 \le K^t_i \le 1 \forall \in i \{1, \dots, dg\} \text{ and } t \in \{1, \dots, Iter\} \qquad (10)$$

After the update of the current limiting factor, the FRT currents of DGs are updated by (11):

$$I^t_{gen(i)} = K^t_i \cdot I_{FRT(i)} \forall \in i \{1, \dots, dg\} \text{ and } t \in \{1, \dots, Iter\} \qquad (11)$$

where $I_{FRT(i)}$ is the FRT current of DG i, as mandated by the standard of each country. Practically, in (11), DGs restrict their current, by a factor K^t_i, to force the objective function (2) to zero, restoring the recloser-fuse coordination.

C. FLOWCHART AND COMPUTATION TIME
The flowchart of the proposed optimization approach is depicted in Fig. 8. It consists of five (5) steps:

Step 1: The iteration index (t) is initialized to $t = 1$. The current limiting factors of all DGs are initialized to 1, e.g., $K^1_i = 1$ for each DG i.

Step 2: The current limiting factor of the best DG that leads the objective function to the greatest decrease, is found in (8).

Step 3: The current limiting factor of the best DG is decreased by dK, using (9).

Step 4: The currents of DGs are calculated in (11), as the product of the mandated FRT currents $\left(I_{FRT(i)}\right)$ and the updated current limiting factors.

Step 5: If the cost function cannot be further reduced, the algorithm is terminated, otherwise it returns to step 2.

Regarding the computation time of the proposed DCD algorithm, steps 1, 3, 4 and 5 involve only a few numerical actions, thus their execution time is negligible. On the other hand, step 2 is a time-consuming step, which involves

multiple SCC to find the optimal action that leads the objective function to the greatest reduction. Specifically, the total number of SCCs of step 2 is given in (12):

$$N_{scc} = 2 \cdot N_{fuses} \cdot N_{DGs} \cdot Iter \quad (12)$$

where N_{scc} is the number of the required SCCs, N_{fuses} is the number of fuses, N_{DGs} is the number of DGs. *Iter* is the total iteration number (e.g., from step 2 to step 5 in the flowchart) until the termination of the algorithm. As an example, let us assume that a network has $N_{fuses} = 10$ fuses and $N_{DGs} = 10$ DGs, while the DCD algorithm requires $Iter = 20$ iterations until convergence. The total SCC number would be $N_{scc} = 2 \cdot 10 \cdot 10 \cdot 20 = 4000$. The computation time of each SCC using superposition-based approaches, e.g., [33], [34], is below 20 ms, even in large networks such as the IEEE 8500-node network. Therefore, the total computation time of the proposed approach is below 80 seconds, which is reasonable.

IV. SIMULATIONS IN THE 13-BUS NETWORK
A. DESCRIPTION OF THE NETWORK
Simulation results are presented here using a modified version of IEEE 13-bus. The examined 13-bus network is shown in Fig. 9, consisting of 9 load buses. Loads are modeled as constant impedances, which is a common and reasonable assumption in SCCs [44]. DGs are connected to buses 4, 11, 13. Five (5) DG penetration scenarios are investigated, as shown in Table 1. Data about the lines and loads are summarized in Table 2.

The protection system consists of two reclosers (RC 1-RC 2) and four fuses (f1-f4) protecting the laterals. RC 1 is coordinated with fuses 1 and 2, while RC 2 with fuses 3 and 4. The time-current curves of RC 1 and fuse 2 are depicted in Fig. 10a. It is noted that in the rest of the paper, the bolted (0 Ohm) fault at the beginning of the lateral and the high impedance (5 Ohm[2]) fault at the end of the lateral are named boundary faults and denoted as "l.i. *lat*" and "h.i. *lat*", respectively, for each lateral *lat*= {1,2,3,4} (see Fig. 9). Due to the symmetry of the network, fuse 1 has the same characteristic as fuse 2 and is not depicted. As shown, in the absence of DGs, the tripping order *fast recloser→fuse→slow recloser* is preserved for all possible faults occurring across the second lateral, namely from a bolted (0 Ohm) fault at the begging of the lateral (e.g., "*l.i.2*") to a high impedance (5 Ohm) fault at the end of the lateral (e.g., "*h.i.2*"). Note that the different currents (1200A and 1000 A) flowing through RC 1 and fuse 2 is due to the load current, which is not negligible in h.i. faults. Contrarily, in l.i. faults, the load current is minimal, since under significant voltage drops, the loads primarily exhibit a constant impedance behavior [44]. The time-current characteristics of RC 2 and fuse 4 are depicted in Fig. 10b. The fuse 3 has the same characteristic as fuse 4 and

---

[2]The range of impedance values cited in literature for high impedance faults varies from 3 Ω [4] to 20 Ω [2]. In this research, we consider 5 Ω. Nonetheless, the proposed method is generic and can be applied for any fault impedance value.
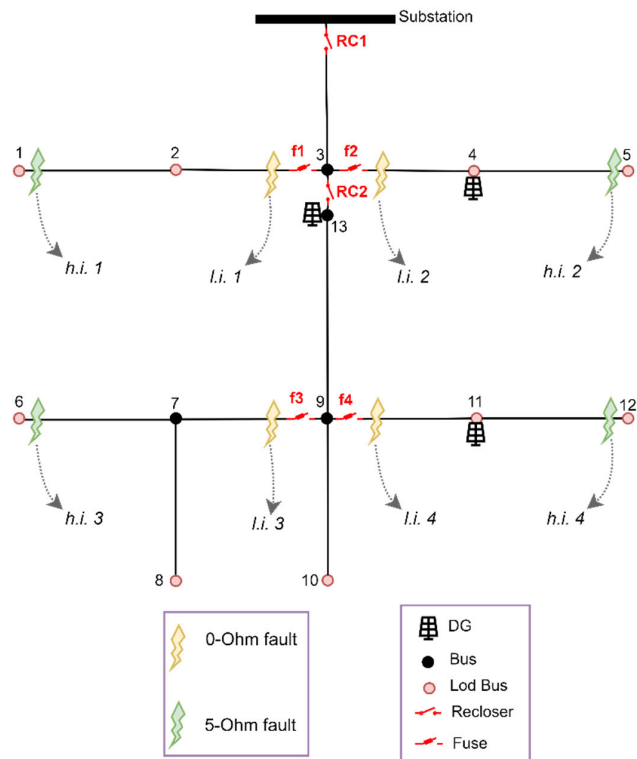

FIGURE 9. Examined 13-Bus Network. The protection system is shown in red. Eight (9) boundary faults are considered.

TABLE 1. DG penetration scenarios.

	DG 4	DG 11	DG 13
Base scenario	0 MW	0 MW	0 MW
Scenario 1	10 MW	0 MW	0 MW
Scenario 2	0 MW	10 MW	0 MW
Scenario 3	0 MW	0 MW	10 MW
Scenario 4	3.5 MW	3.5 MW	3.5 MW
Scenario 5	2 MW	2 MW	2 MW

is not depicted. The coordination is preserved for all possible faults within the fourth lateral, namely from the "h.i. 4" to the "l.i. 4" fault. Data about the settings of protection equipment are summarized in Table 2.

The integration of DGs restricts the coordination region as explained in section II. The proposed approach is compared against the following methods, assuming the 5 scenarios of Table 1.

- DGs inject a current according to the German FRT code, which is mathematically given by (1) (refer to Section II-A), without any limitation of the DG current.
- DGs inject a current according to the German FRT code. However, their current is restricted by multiplying it with a current limiting factor (CLF) proposed by Yazdanpanahi in [29, eq. (10)]. The CLF is given in (13).

$$CLF = \begin{cases} 1.4674 \cdot R_{pcc(i)}^3 & if \ R_{pcc(i)} < 0.9 \\ 1 & otherwise \end{cases} \quad (13)$$

TABLE 2. 13-bus network's parameters.

Nominal Phase to-Neutral Voltage		7200 V
Resistance of the lines		0.119 Ohm/km
Self-Reactance of the lines		0.25 Ohm/km
Mutual-Reactance of the lines		0.08 Ohm/km
Max. line current		357 A
Line length between buses 3-13 Line length between buses 13-9 All the other lines		0.1 km 12 km 5 km
Load Buses		1, 2, 4, 5, 6, 8, 10, 11, 12
Constant impedance load per phase		200 // 800j Ohm
Total Load Power		7 MW
Recloser 1	TDS fast curve	1.3
	TDS slow curve	8.1
	Peak up current	220 A
	Characteristic of relay	IEEE Extremely inverse [16]
Recloser 2	TDS fast curve	0.6
	TDS slow curve	1.2
	Peak up current	120 A
	Characteristic of relay	IEEE Extremely inverse [16]
Fuses 1, 2	a	-1.8 [45]
	b	6.3236 [45]
Fuses 3, 4	a	-1.8 [12]
	b	5.1196 [12]

Essentially, the current limitation is most pronounced in DGs experiencing higher voltage drops, namely those located near the fault location.

- The same with the previous case, but instead, the current is limited by the CLF of Fani [18, eq. (6)], as follows:

$$CLF = \begin{cases} R_{pcc(i)}^{\frac{1}{R_{pcc(i)}}} & if\ R_{pcc(i)} < 0.9 \\ 1 & otherwise \end{cases} \quad (14)$$

B. SCENARIO 1 (DG 4)

In this scenario, a DG of 10 MW is connected to bus 4 as shown in Fig. 9. The CLFs calculated by the compared methods, for all boundary faults of Fig. 9, are depicted in Fig. 11. Moreover, the effectiveness of the compared method in preserving the recloser-fuse coordination is quoted in Table 3. As shown, only the proposed method preserves the coordination in the "*h.i. 2*" fault. It is because the voltage experienced by DG 4 during the "*h.i. 2*" fault is high (6000 V at bus 4), and thus, the CLF in equations (13) and (14) is not sufficiently low to prevent the miscoordination. Specifically, as shown in Fig. 11, the CLF of the "*h.i.2*" fault is 0.4 for the proposed method; in contrast, Yazdanpanahi's and Fani's method yield a CLF for the same fault equal to 0.82 and 0.73, respectively, which are not adequate to prevent the miscoordination.

Fig. 12 presents the shift of tripping times of slow recloser 1 and fuse 2, for the "*h.i. 2*" fault, due to the DG 4. As shown in Fig. 12a, without (w/o) the DG, the fuse 2 trips at 8.35 s, namely before the slow RC 1 that trips at 8.72 s. The connection of DG 4 blinds both fuse 2 and RC 1, shifting their tripping time to 17.2 s and 15.6 s, respectively; thus,
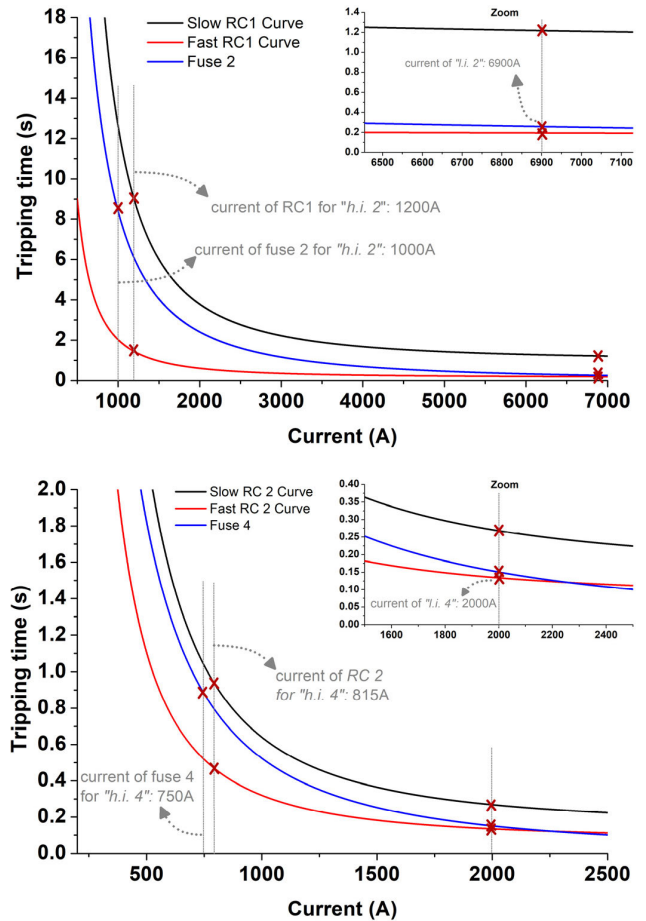

FIGURE 10. From top to bottom: Time current curves of a) recloser 1-fuse 2, and b) recloser 2-fuse 4, for the base scenario (no DGs).

TABLE 3. Coordination of boundary faults for scenario 1 (✓coordination, ✗miscoordination).

	h.i. 1	l.i. 1	h.i. 2	l.i. 2	h.i. 3	l.i. 3	h.i. 4	l.i. 4
German FRT	✓	✓	✗	✓	✓	✓	✓	✓
Proposed	✓	✓	✓	✓	✓	✓	✓	✓
Yazdanpanahi	✓	✓	✗	✓	✓	✓	✓	✓
Fani	✓	✓	✗	✓	✓	✓	✓	✓

the coordination is lost since fuse 2 trips before the slow recloser. This type of miscoordination is similar to "*type 4 miscoordination*", according to the classification presented in section II. The issue of miscoordination is not resolved either by the Yazdanpanahi's or the Fani's methods, as confirmed in Figs. 12b and 12c. On the contrary, the proposed method sufficiently restricts the FRT current of DG (CLF=0.4), preventing miscoordination.

Looking at Fig. 11, the proposed approach calculates the CLF based on the worst-case condition (namely "*h.i. 2*") and imposes it on the DG for all faults, even in those without mis-coordination issues such as the "*h.i. 1*". It is because without the use of real-time monitoring and fault location identification functionalities, DGs cannot distinguish the position of the fault; for instance, DG cannot distinguish whether a fault
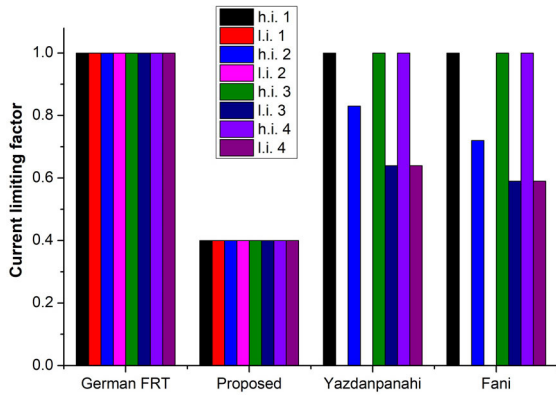
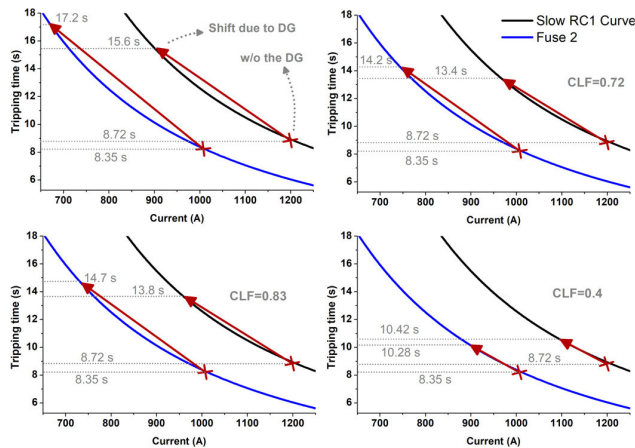**FIGURE 11.** Current limiting factors of the examined methods, for scenario 1.

FIGURE 12. Fault "*h.i.* 2" of scenario 1: a) German FRT (top-left), b) Fani (top-right), c) Yazdanpanahi (bottom-left), d) proposed (bottom-right).

is "*h.i. 2*" or "*h.i. 1*", thus it takes the worst-case condition to be on the safe side. It is a rather conservative approach, which however always guarantees recloser-fuse coordination, for all boundary faults, without advanced communication means.

C. SCENARIO 2 (DG 11)

In this scenario, a DG of 10 MW is connected to bus 11. The CLF of the compared methods and their coordination, for all boundary faults, are quoted in Fig. 13 and Table 4, respectively. Only the proposed method ensures coordination for all boundary faults. Fani's method loses the coordination in "*h.i. 3*" and "*h.i. 4*", while Yazdanpanahi's in "*h.i. 4*" fault, owing to their high CLF values. For example, as shown in Fig. 13, Fani's and Yazdanpanahi's methods yield CLF values 0.49 and 0.33, respectively, for the "*h.i. 4*" fault, which are not sufficient to prevent miscoordination.

The shift of tripping times of fuse 3 and recloser 2, due to DG 11, for the "*h.i. 3*" fault, is depicted in Fig. 14. As shown in Fig. 14a, without current limitation, the coordination is lost, as the fuse trips (at 0.63 s) before the fast recloser (at 1 s). This type of miscoordination is the "*type 2 miscoordination*" of the classification of section II-B. Fani's method does not effectively restore coordination, in contrast to the proposed and Yazdanpanahi's method.

TABLE 4. Coordination of boundary faults for scenario 2.

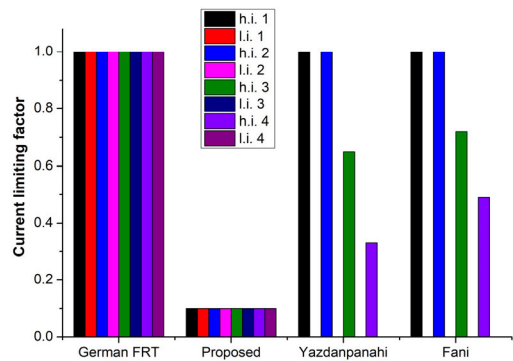|	h.i. 1	l.i. 1	h.i. 2	l.i. 2	h.i. 3	l.i. 3	h.i. 4	l.i. 4
German FRT	✓	✓	✓	✓	✗	✗	✗	✓
Proposed	✓	✓	✓	✓	✓	✓	✓	✓
Yazdanpanahi	✓	✓	✓	✓	✓	✓	✗	✓
Fani	✓	✓	✓	✓	✗	✓	✗	✓

FIGURE 13. Current limiting factors of the examined methods, for scenario 2.
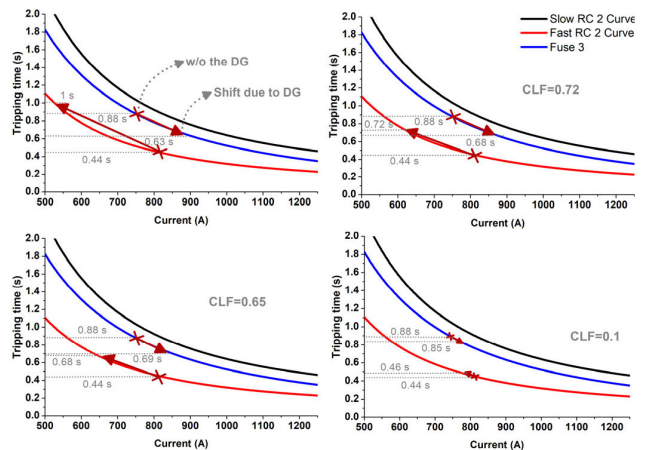

FIGURE 14. Fault "*h.i. 3*" of scenario 2: a) German FRT (top-left), b) Fani (top-right), c) Yazdanpanahi (bottom-left), d) proposed (bottom-right).

The shift of tripping times of fuse 4 and recloser 2, due to DG 11, for the "*h.i. 4*" fault, is depicted in Fig. 15. As shown in Fig. 15a, the presence of DG disrupts the coordination between fuse 4 and slow RC 2, since the slow recloser trips (at 1.3 s) before the fuse (at 1.4 s). Only the proposed method achieves coordination restoration, as depicted in Fig. 15d. It is noted that, for the sake of clarity, the CTI between the curves has been ignored here. However, the objective function (2) can be easily expanded to include CTI, ensuring a sufficient margin, e.g., 50ms, between the fuse and recloser (refer to Appendix for expansion).

D. SCENARIO 3 (DG 13)

In this scenario, a DG of 10 MW is connected to bus 13. The CLF of the compared methods and their coordination, for all boundary faults, are quoted in Fig. 16 and Table 5, respectively. As shown in the table, miscoordination is observed
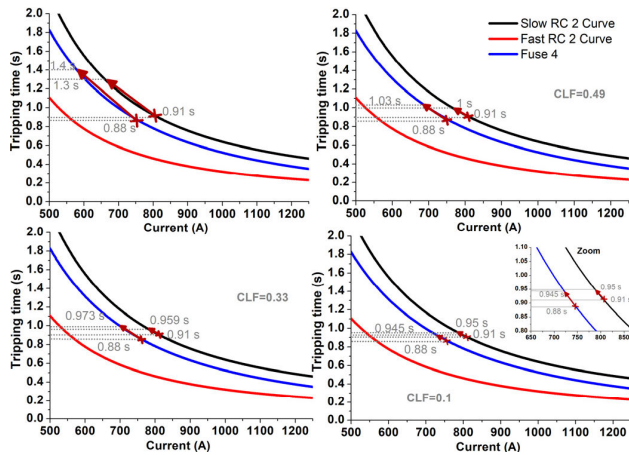
FIGURE 15. Fault "*h.i.* 4" of scenario 2: a) German FRT (top-left), b) Fani (top-right), c) Yazdanpanahi (bottom-left), d) proposed (bottom-right).

TABLE 5. Coordination of boundary faults for scenario 3.

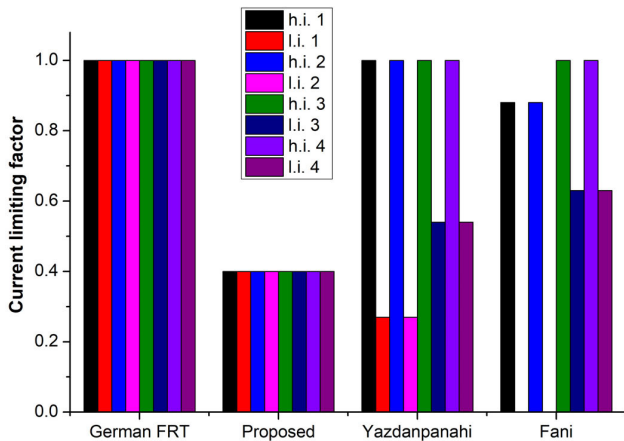|	h.i. 1	l.i. 1	h.i. 2	l.i. 2	h.i. 3	l.i. 3	h.i. 4	l.i. 4
German FRT	✓	✓	✓	✓	✗	✗	✗	✗
Proposed	✓	✓	✓	✓	✓	✓	✓	✓
Yazdanpanahi	✓	✓	✓	✓	✗	✗	✗	✗
Fani	✓	✓	✓	✓	✗	✗	✗	✗

FIGURE 16. Current limiting factors of the examined methods, for scenario 3.

in "*h.i. 3*", "*l.i. 3*", "*h.i. 4*", "*l.i. 4*" faults, which is not effectively treated by the Yazdanpanahi's and Fani's methods. Specifically, DG 13 is located far away from those faults (line 13-9 is long), experiencing only a slight voltage drop. Therefore, according to (13)-(14), Yazdanpanahi's and Fani's methods yield high CLF values, failing to prevent miscoordination.

Fig. 17 depicts the shift of tripping times of fast RC 2- fuse 4 for the "*l.i. 4*" fault. As shown in Fig. 17a, the DG shifts the tripping time of fuse 4 from 0.15 s to 0.13 s, and fast RC 2 from 0.13 s to 0.16 s, disrupting their coordination. It is the "*type 3 miscoordination*" described in section II. The miscoordination remains in Figs 17b and 17c as well, while solved only by the proposed approach in Fig. 17d.
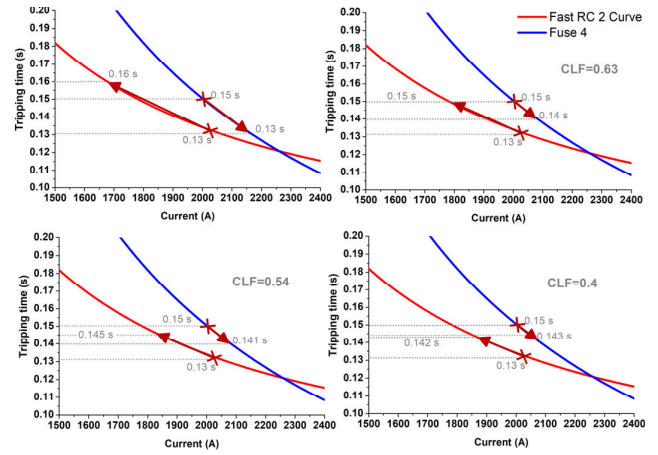

FIGURE 17. Fault "*l.i.* 4" of scenario 3: a) German FRT (top-left), b) Fani (top-right), c) Yazdanpanahi (bottom-left), d) proposed (bottom-right).

TABLE 6. Coordination of boundary faults for scenario 4.

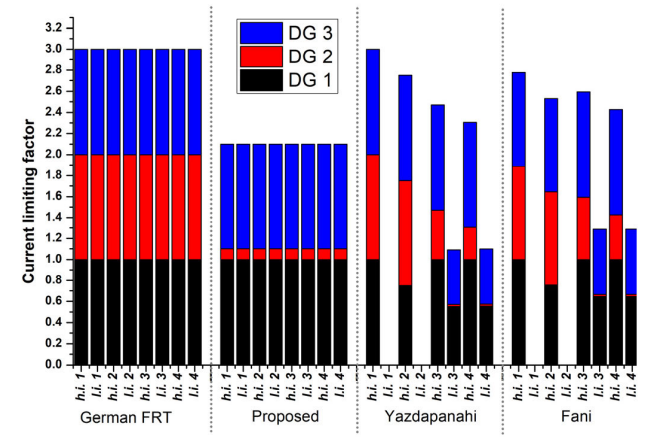|	h.i. 1	l.i. 1	h.i. 2	l.i. 2	h.i. 3	l.i. 3	h.i. 4	l.i. 4
German FRT	✓	✓	✓	✓	✗	✗	✓	✓
Proposed	✓	✓	✓	✓	✓	✓	✓	✓
Yazdanpanahi	✓	✓	✓	✓	✓	✓	✓	✓
Fani	✓	✓	✓	✓	✓	✓	✓	✓

FIGURE 18. Current limiting factors of the examined methods, for scenario 4.

E. SCENARIO 4

In this scenario, three DGs of 3.5 MW are connected. The CLFs of DGs and the coordination for all boundary faults are quoted in Fig. 18 and Table 6, respectively. As shown in the table, miscoordination occurs in "*h.i. 3*" and "*l.i. 3*" faults, which are effectively treated by all methods. An important thing to note in Fig. 18 is that the proposed method offers a better FRT current support (higher CLFs) than the Yazdanpanahi's and Fani's methods in all low-impedance faults. For example, in "*l.i. 3*" fault, the CLF of the DG 4, 11 and 13 are estimated by the proposed method as 1, 0.1 and 1, respectively, while the respective factors of Yazdanpanahi's method are 0.55, 0 and 0.52. This property is a strong advantage of the proposed method, since the

TABLE 7. Coordination of boundary faults for scenario 5.

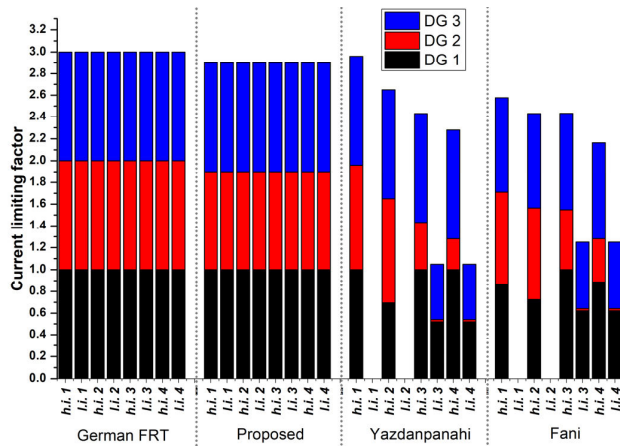|	h.i. 1	l.i. 1	h.i. 2	l.i. 2	h.i. 3	l.i. 3	h.i. 4	l.i. 4
German FRT	✓	✓	✓	✓	✓	✗	✓	✓
Proposed	✓	✓	✓	✓	✓	✓	✓	✓
Yazdanpanahi	✓	✓	✓	✓	✓	✓	✓	✓
Fani	✓	✓	✓	✓	✓	✓	✓	✓

FIGURE 19. Current limiting factors of the examined methods, for scenario 5.

medium-voltage (MV), and especially the upstream high-voltage (HV) network has a higher need for reactive power support by DGs in low impedance faults, to enhance their voltage stability.

F. SCENARIO 5

In this scenario, three DGs of 2 MW are connected. The CLF of DGs and the coordination for all boundary faults are quoted in Fig. 19 and Table 7, respectively. Only the "*l.i. 3*" fault causes miscoordination in this scenario, which is effectively treated by all methods. The CLF of the three DGs are estimated by the proposed method as 1, 0.9, 1. In this scenario, the proposed method yields high CLFs due to the low power of DGs (2 MW), which causes only minor coordination issues that are addressed with a slight reduction of CLFs. It is worth noting in Fig. 19 that the proposed method offers a much better reactive power support than the Yazdanpanahi's and Fani's methods in all faults (except the "*h.i.1*").

V. SIMULATIONS ON THE IEEE 8500-NODE NETWORK

This section presents simulation results in the IEEE 8500-node network shown in Fig. 20. It is a real north American network, supplying 2521 buses with a total power 10.5 MW [46]. The original network has been slightly modified to include 4 DGs with FRT capability according to (1), two reclosers protecting the two feeders, and three fuses. RC 1 is coordinated with fuse 1 to protect the first feeder, while RC 2 with fuses 2 and 3 to protect the second feeder. All the data of the network, DGs, and PDs are shown in Table 8. DG 1 and 2 are located between the RC 1 and fuse 1, DG 3 is
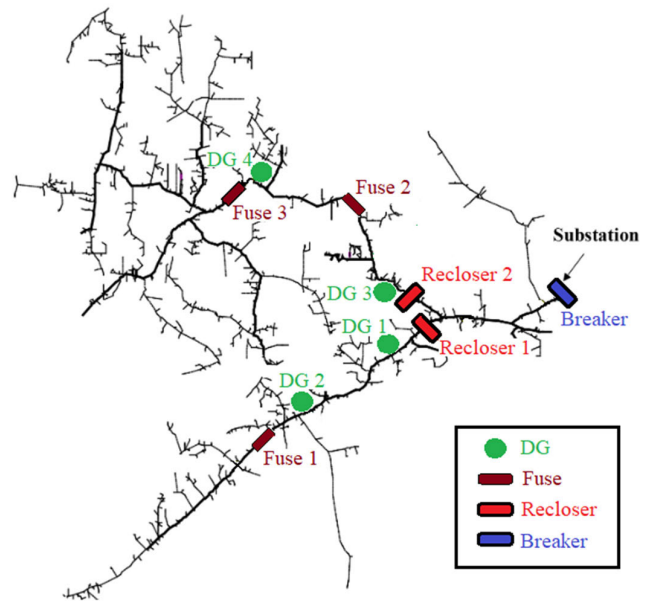

FIGURE 20. IEEE 8500-Node network, including 1 breaker, 2 reclosers, 3 fuses and 4 DGs.

TABLE 8. IEEE 8500-node network's parameters.

Nominal Phase to-Neutral Voltage		7200 V
Data of Lines		See in [46]
Maximum load		10.5 MW
Power of DG i = {1, 2, 3, 4}		2.5 MW, 1 MW, 3 MW, 3 MW
Recloser 1	TDS fast curve	0.1
	TDS slow curve	0.3
	Peak up current	300 A
	Characteristic of relay	IEEE Extremely inverse [16]
Recloser 2	TDS fast curve	0.1
	TDS slow curve	0.5
	Peak up current	500 A
	Characteristic of relay	IEEE Extremely inverse [16]
Fuse 1	a	-1.8 [12]
	b	5.1196 [1]
Fuse 2	a	-1.8 [1]
	b	5.75 [1]
Fuse 3	a	-1.8 [12]
	b	5.5309 [12]

between RC 2 and fuse 2, while DG 4 is between the fuse 2 and fuse 3.

Fig. 21a depicts the time-current curves of RC 1-fuse 1 pair, where "*h.i. 1*" and "*l.i. 1*" denote respectively a high impedance (5 Ohm) and a bolted (0 Ohm) fault downstream of the fuse 1. As shown, in the absence of DGs, coordination is achieved for all faults downstream of the fuse 1 (between 560A and 906A). Fig. 21b depicts the time-current curves of RC 2- fuse 2- fuse 3, where the tripping order of fast RC 2 → fuse 3 → fuse 2 → slow RC 2 is valid for all currents downstream of the fuse 3, namely from 900 A to 1530 A. Moreover, coordination is accomplished for all faults between fuse 2 and fuse 3 (from 1100A to 2170A), with a tripping order fast RC 2 → fuse 2 → slow RC 2. Subsequently,
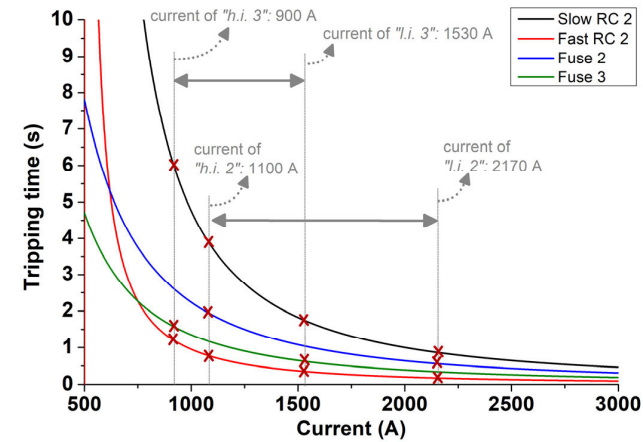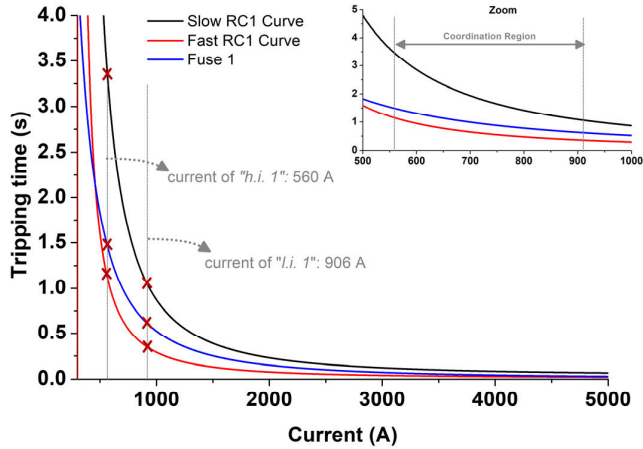
FIGURE 21. From top to bottom: Time current curves of a) recloser 1-fuse 1, and b) recloser 2- fuse 2- fuse 3, without the DGs.

TABLE 9. Coordination of boundary faults for IEEE 8500-node network.

	h.i. 1	l.i. 1	h.i. 2	l.i. 2	h.i. 3	l.i. 3
German FRT	✗	✓	✓	✓	✗	✓
Proposed	✓	✓	✓	✓	✓	✓
Yazdanpanahi	✗	✓	✓	✓	✓	✓
Fani	✗	✓	✓	✓	✓	✓

we investigate the impact of DGs on PD coordination, comparing various FRT methods outlined in Section IV-A, including German FRT (equation 1) without limitation, the proposed, Yazdanpanahi's, and Fani's methods. The powers of DG are given in Table 8.

Table 9 and Fig. 22 depict respectively the PD coordination and the CLFs of the compared methods, for all boundary faults. As shown in the table, the German FRT disrupts the coordination for both the "h.i.1" and "h.i.3" faults. Specifically, for "h.i.1", DG 1 and 2 blind the RC 1, while speeding up the tripping time of fuse 1; thus, the fuse 1 trips before the fast RC 1, disrupting their coordination. As indicated in the table, the decentralized current limiting methods of Yazdanpanahi and Fani fail to prevent miscoordination in the "h.i.1" fault. This occurs because DG 1 is situated
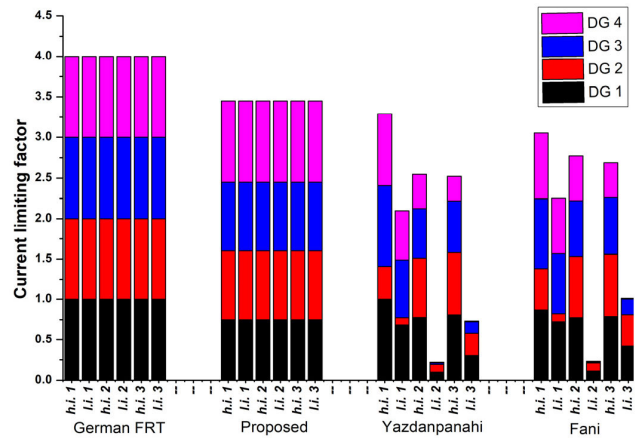

FIGURE 22. Current limiting factors of the DGs for the IEEE 8500-node network.
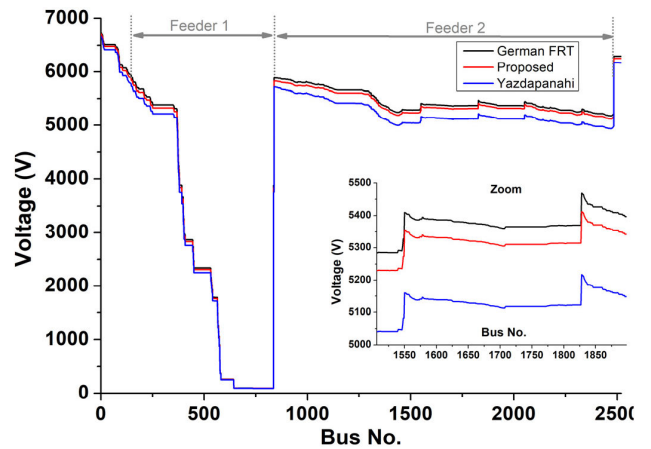

FIGURE 23. Voltage profile (phase A) of the compared methods, for the "l.i.1" fault.

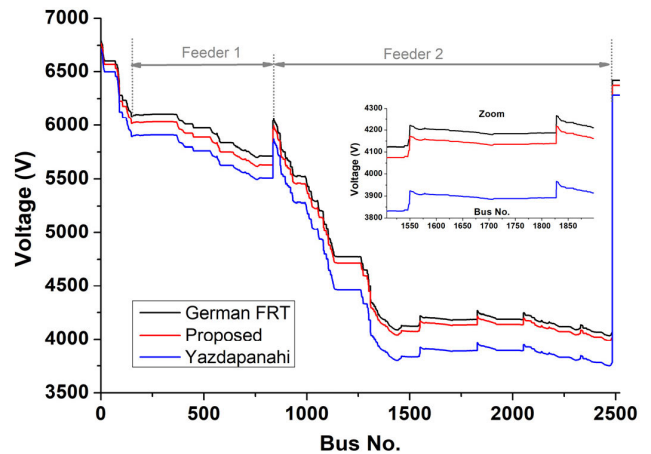

FIGURE 24. Voltage profile (phase A) of the compared methods, for the "h.i.3" fault.

at a considerable distance from the "h.i.1" fault, resulting in only a minor voltage drop and a slight CLF reduction (refer to Fig. 22), which does not suffice to prevent the miscoordination between RC 1 and fuse 1. Conversely, our proposed method ensures coordination under all boundary fault conditions.

Figures 23 and 24 display the voltage profiles of the IEEE 8500-node network for the "*l.i.1*" and "*h.i.3*" faults, respectively. For clarity, we have represented only phase A, with similar characteristics observed in the other phases as well. It is worth noting that the voltage profile of Fani's method closely resembles that of Yazdanpanahi's and is therefore not separately depicted. Within both figures, it is evident that the German FRT exhibits the highest voltage profile during the faults. This superiority arises from the absence of limitations imposed on the DGs, as evidenced by a CLF of 1 for all DGs in Fig. 22. In contrast, our proposed method outperforms Yazdanpanahi's approach, as shown in Figs. 23-24, thanks to the higher CLF imposed on the DGs. In summary, the proposed method surpasses decentralized methods in both PD coordination and voltage support during faults.

VI. CONCLUSION

In this paper, we introduce a straightforward discrete coordinate-descent approach aimed at optimizing the FRT behavior of DGs to prevent miscoordination between reclosers and fuses. Our method begins by calculating DG fault currents based on the specific FRT standard of each country. If any miscoordination between reclosers and fuses is identified, the method intelligently scales down the current of DGs, until proper coordination is reestablished. The proposed approach boasts minimal communication requirements, reasonable computational efficiency, and reliable voltage support during fault conditions. Through simulations conducted on both the IEEE 13-bus and IEEE 8500-node systems, our approach consistently maintains recloser-fuse coordination in all the examined cases and offers superior voltage support during faults compared to the decentralized current limiting strategies.

APPENDIX

Objective function (2) can be easily expanded to include multiple fuses, and the CTI between the fuse and recloser curves, as follows:

$$
\begin{aligned}
f = \sum_{p=1}^{N_{fuse}} & \left(T^t_{f_p,hi} - T^t_{rc_p,sl \to f_p,hi} + CTI \right)^2 \\
& \cdot \mathrm{H} \left(T^t_{f_p,hi} - T^t_{rc_p,sl \to f_p,hi} + CTI \right) \\
+ \sum_{p=1}^{N_{fuse}} & \left(T^t_{rc_p,fa \to f_p,hi} - T^t_{f_p,hi} + CTI \right)^2 \\
& \cdot \mathrm{H} \left(T^t_{rc_p,fa \to f_p,hi} - T^t_{f_p,hi} + CTI \right) \\
+ \sum_{p=1}^{N_{fuse}} & \left(T^t_{rc_p,fa \to f_p,li} - T^t_{f_p,li} + CTI \right)^2 \\
& \cdot \mathrm{H} \left(T^t_{rc_p,fa \to f_p,li} - T^t_{f_p,li} + CTI \right)
\end{aligned}
$$

where N_{fuse} is the number of fuses, $T^t_{f_p,hi}$ is the tripping time of pth fuse for a high impedance fault downstream the fuse,

$T^t_{rc_p,sl \to f_p,hi}$ is the tripping time of the slow recloser for a high impedance fault downstream the pth fuse etc.

REFERENCES

[1] S. Jamali and H. Borhani-Bahabadi, "Recloser time–current–voltage characteristic for fuse saving in distribution networks with DG," *IET Gener., Transmiss. Distrib.*, vol. 11, no. 1, pp. 272–279, Jan. 2017.

[2] H. Bisheh, B. Fani, G. Shahgholian, I. Sadeghkhani, and J. M. Guerrero, "An adaptive fuse-saving protection scheme for active distribution networks," *Int. J. Electr. Power Energy Syst.*, vol. 144, Jan. 2023, Art. no. 108625.

[3] L. Strezoski, I. Stefani, and D. Bekut, "Novel method for adaptive relay protection in distribution systems with electronically-coupled DERs," *Int. J. Electr. Power Energy Syst.*, vol. 116, Mar. 2020, Art. no. 105551.

[4] M. Yousaf, A. Jalilian, K. M. Muttaqi, and D. Sutanto, "An adaptive overcurrent protection scheme for dual-setting directional recloser and fuse coordination in unbalanced distribution networks with distributed generation," *IEEE Trans. Ind. Appl.*, vol. 58, no. 2, pp. 1831–1842, Mar. 2022.

[5] C. Reiz and J. B. Leite, "Optimal coordination of protection devices in distribution networks with distributed energy resources and microgrids," *IEEE Access*, vol. 10, pp. 99584–99594, 2022.

[6] *IEEE Standard for Interconnecting Distributed Resources With Electric Power Systems*, IEEE Standard 1547-2003, 2003, p. 7.

[7] M. H. Sadeghi, A. Dastfan, and Y. Damchi, "Optimal distributed generation penetration considering relay coordination and power quality requirements," *IET Gener., Transmiss. Distribution*, vol. 16, no. 12, pp. 2466–2475, Jun. 2022.

[8] H. A. Abdel-Ghany, A. M. Azmy, N. I. Elkalashy, and E. M. Rashad, "Optimizing DG penetration in distribution networks concerning protection schemes and technical impact," *Electric Power Syst. Res.*, vol. 128, pp. 113–122, Nov. 2015.

[9] H. Zhan, C. Wang, Y. Wang, X. Yang, X. Zhang, C. Wu, and Y. Chen, "Relay protection coordination integrated optimal placement and sizing of distributed generation sources in distribution networks," *IEEE Trans. Smart Grid*, vol. 7, no. 1, pp. 55–65, Jan. 2016.

[10] A. Heidary, H. Radmanesh, K. Rouzbehi, A. Mehrizi-Sani, and G. B. Gharehpetian, "Inductive fault current limiters: A review," *Electric Power Syst. Res.*, vol. 187, Oct. 2020, Art. no. 106499.

[11] A. Safaei, M. Zolfaghari, M. Gilvanejad, and G. B. Gharehpetian, "A survey on fault current limiters: Development and technical aspects," *Int. J. Electr. Power Energy Syst.*, vol. 118, Jun. 2020, Art. no. 105729.

[12] S. Chaitusaney and A. Yokoyama, "Prevention of reliability degradation from recloser–fuse miscoordination due to distributed generation," *IEEE Trans. Power Del.*, vol. 23, no. 4, pp. 2545–2554, Oct. 2008.

[13] P. H. A. Barra, D. V. Coury, and R. A. S. Fernandes, "A survey on adaptive protection of microgrids and distribution systems with distributed generators," *Renew. Sustain. Energy Rev.*, vol. 118, Feb. 2020, Art. no. 109524.

[14] H. Lin, K. Sun, Z. Tan, C. Liu, J. M. Guerrero, and J. C. Vasquez, "Adaptive protection combined with machine learning for microgrids," *IET Gener., Transmiss. Distribution*, vol. 13, no. 6, pp. 770–779, Mar. 2019.

[15] M. C. Vargas, O. E. Batista, and Y. Yang, "Estimation method of short-circuit current contribution of inverter-based resources for symmetrical faults," *Energies*, vol. 16, no. 7, p. 3130, Mar. 2023.

[16] M. Al Talaq and M. Al-Muhaini, "Optimal coordination of time delay overcurrent relays for power systems with integrated renewable energy sources," *Energies*, vol. 15, no. 18, p. 6749, Sep. 2022.

[17] K. Pereira, B. R. Pereira, J. Contreras, and J. R. S. Mantovani, "A multiobjective optimization technique to develop protection systems of distribution networks with distributed generation," *IEEE Trans. Power Syst.*, vol. 33, no. 6, pp. 7064–7075, Nov. 2018.

[18] B. Fani, F. Hajimohammadi, M. Moazzami, and M. J. Morshed, "An adaptive current limiting strategy to prevent fuse-recloser miscoordination in PV-dominated distribution feeders," *Electric Power Syst. Res.*, vol. 157, pp. 177–186, Apr. 2018.

[19] S. I. Gkavanoudis, D. Tampakis, K. D. Malamaki, G. C. Kryonidis, E. O. Kontis, K. O. Oureilidis, J. M. Maza-Ortega, and C. S. Demoulias, "Protection philosophy in low short-circuit capacity distribution grids with high penetration of converter-interfaced distributed renewable energy sources," *IET Gener., Transmiss. Distribution*, vol. 14, no. 22, pp. 4978–4988, Nov. 2020.

[20] H. F. Habib, C. R. Lashway, and O. A. Mohammed, "A review of communication failure impacts on adaptive microgrid protection schemes and the use of energy storage as a contingency," *IEEE Trans. Ind. Appl.*, vol. 54, no. 2, pp. 1194–1207, Mar. 2018.

[21] A. M. Tsimtsios, A. S. Safigianni, and V. C. Nikolaidis, "Generalized distance-based protection design for DG integrated MV radial distribution networks—Part I: Guidelines," *Electr. Power Syst. Res.*, vol. 176, Nov. 2019, Art. no. 105949.

[22] W. Li, Y. Tan, Y. Li, Y. Cao, C. Chen, and M. Zhang, "A new differential backup protection strategy for smart distribution networks: A fast and reliable approach," *IEEE Access*, vol. 7, pp. 38135–38145, 2019.

[23] E. Casagrande, W. L. Woon, H. H. Zeineldin, and D. Svetinovic, "A differential sequence component protection scheme for microgrids with inverter-based distributed generators," *IEEE Trans. Smart Grid*, vol. 5, no. 1, pp. 29–37, Jan. 2014.

[24] E. Ebrahimi, M. J. Sanjari, and G. B. Gharehpetian, "Control of three-phase inverter-based DG system during fault condition without changing protection coordination," *Int. J. Electr. Power Energy Syst.*, vol. 63, pp. 814–823, Dec. 2014.

[25] N. Rajaei, M. H. Ahmed, M. M. A. Salama, and R. K. Varma, "Fault current management using inverter-based distributed generators in smart grids," *IEEE Trans. Smart Grid*, vol. 5, no. 5, pp. 2183–2193, Sep. 2014.

[26] W. Kou and D. Wei, "Fault ride through strategy of inverter-interfaced microgrids embedded in distributed network considering fault current management," *Sustain. Energy, Grids Netw.*, vol. 15, pp. 43–52, Sep. 2018.

[27] X. Liu, C. Li, M. Shahidehpour, Y. Gao, B. Zhou, Y. Zhang, J. Yi, and Y. Cao, "Fault current hierarchical limitation strategy for fault ride-through scheme of microgrid," *IEEE Trans. Smart Grid*, vol. 10, no. 6, pp. 6566–6579, Nov. 2019.

[28] M. A. Gabr, R. A. El-Sehiemy, T. F. Megahed, Y. Ebihara, and S. M. Abdelkader, "Optimal settings of multiple inverter-based distributed generation for restoring coordination of DOCRs in mesh distribution networks," *Electr. Power Syst. Res.*, vol. 213, Dec. 2022, Art. no. 108757.

[29] H. Yazdanpanahi, Y. W. Li, and W. Xu, "A new control strategy to mitigate the impact of inverter-based DGs on protection system," *IEEE Trans. Smart Grid*, vol. 3, no. 3, pp. 1427–1436, Sep. 2012.

[30] P. E. Muñoz, R. J. Mantz, and S. A. González, "Control-based fault current limiter for minimizing impact of distributed generation units on protection systems," *J. Modern Power Syst. Clean Energy*, vol. 11, no. 2, pp. 643–650, Mar. 2023.

[31] C. Su, Z. Liu, Z. Chen, and Y. Hu, "An adaptive control strategy of converter-based DG to maintain protection coordination in distribution system," in *Proc. IEEE PES Innov. Smart Grid Technol.*, Istanbul, Turkey, 2014, pp. 1–6.

[32] M. M. Salem, N. I. Elkalashy, Y. Atia, and T. A. Kawady, "Modified inverter control of distributed generation for enhanced relaying coordination in distribution networks," *IEEE Trans. Power Del.*, vol. 32, no. 1, pp. 78–87, Feb. 2017.

[33] E. E. Pompodakis, L. Strezoski, N. Simic, A. G. Paspatis, M. C. Alexiadis, A. G. Tsikalakis, Y. A. Katsigiannis, and E. S. Karapidakis, "Short-circuit calculation of droop-controlled islanded AC microgrids with virtual impedance current limiters," *Electric Power Syst. Res.*, vol. 218, May 2023, Art. no. 109184.

[34] J. He, Z. Li, W. Li, J. Zou, X. Li, and F. Wu, "Fast short-circuit current calculation of unbalanced distribution networks with inverter-interfaced distributed generators," *Int. J. Electr. Power Energy Syst.*, vol. 146, Mar. 2023, Art. no. 108728.

[35] S. Vadari, I. Džafic, D. Koch, R. Murphy, D. Hayes, and T. Donlagic, "Distribution control centers in the US and Europe: Commonalities, differences, and lessons," *J. Modern Power Syst. Clean Energy*, vol. 10, no. 2, pp. 259–268, Mar. 2022.

[36] R. A. Jabr and I. Džafic, "Sensitivity-based discrete coordinate-descent for volt/VAr control in distribution networks," *IEEE Trans. Power Syst.*, vol. 31, no. 6, pp. 4670–4678, Nov. 2016.

[37] R. A. Jabr and I. Džafic, "Distribution management systems for smart grid: Architecture, work flows, and interoperability," *J. Modern Power Syst. Clean Energy*, vol. 10, no. 2, pp. 300–308, Mar. 2022.

[38] R. A. J. Amalorpavaraj, P. Kaliannan, S. Padmanaban, U. Subramaniam, and V. K. Ramachandaramurthy, "Improved fault ride through capability in DFIG based wind turbines using dynamic voltage restorer with combined feed-forward and feed-back control," *IEEE Access*, vol. 5, pp. 20494–20503, 2017.

[39] J. Jia, G. Yang, and A. H. Nielsen, "A review on grid-connected converter control for short-circuit power provision under grid unbalanced faults," *IEEE Trans. Power Del.*, vol. 33, no. 2, pp. 649–661, Apr. 2018.

[40] M. M. Shabestary, S. Mortazavian, and Y. A-R. I. Mohamed, "Asymmetric low-voltage ride-through scheme and dynamic voltage regulation in distributed generation units," in *Proc. IEEE Appl. Power Electron. Conf. Exposit. (APEC)*, San Antonio, TX, USA, Mar. 2018, pp. 1603–1608.

[41] A. Azizi, A. Banaiemoqadam, A. Hooshyar, and M. Patel, "A blind spot in the LVRT current requirements of modern grid codes for inverter-based resources," *IEEE Trans. Power Del.*, vol. 38, no. 1, pp. 319–334, Feb. 2023.

[42] D. Z. Farsa and S. Rahnamayan, "Discrete coordinate descent (DCD)," in *Proc. IEEE Int. Conf. Syst., Man, Cybern. (SMC)*, Toronto, ON, Canada, Oct. 2020, pp. 184–190.

[43] H. Fang, G. Fang, T. Yu, and P. Li, "Efficient greedy coordinate descent via variable partitioning," in *Proc. 37th Conf. Uncertainty Artif. Intell. (UAI)*, 2021, pp. 547–557.

[44] A. Bokhari, A. Alkan, R. Dogan, M. Diaz-Aguiló, F. de León, D. Czarkowski, Z. Zabar, L. Birenbaum, A. Noel, and R. E. Uosef, "Experimental determination of the ZIP coefficients for modern residential, commercial, and industrial loads," *IEEE Trans. Power Del.*, vol. 29, no. 3, pp. 1372–1381, Jun. 2014.

[45] A. F. Naiem, Y. Hegazy, A. Y. Abdelaziz, and M. A. Elsharkawy, "A classification technique for recloser-fuse coordination in distribution systems with distributed generation," *IEEE Trans. Power Del.*, vol. 27, no. 1, pp. 176–185, Jan. 2012.

[46] IEEE PES Distribution Test Feeders. (Oct. 2023). *8500-Node Test Feeder*. [Online]. Available: https://cmte.ieee.org/pes-testfeeders/resource

EVANGELOS E. POMPODAKIS received the Diploma degree from the School of Electrical and Computer Engineering, Aristotle University of Thessaloniki, Thessaloniki, Greece, in 2011, the master's degree from the Technical University of Kaiserslautern, Kaiserslautern, Germany, in 2015, and the Ph.D. degree from the Aristotle University of Thessaloniki, in 2021. He is currently a Postdoctoral Researcher with Hellenic Mediterranean University, Crete, Greece. His research interests include distribution system modeling, power converters, power system protection, smart grids, and microgrids.

YIANNIS A. KATSIGIANNIS received the Diploma degree in production engineering and management, the Diploma degree in environmental engineering, the M.Sc. and Ph.D. degrees from the Technical University of Crete. He is currently an Assistant Professor of renewable energy systems optimization with the Department of Electrical and Computer Engineering, Hellenic Mediterranean University (HMU). His research interests include renewable energy sources and their integration to power systems, autonomous power systems, small- and large-scale energy storage, smart grids, energy saving, and artificial intelligence.

EMMANOUEL S. KARAPIDAKIS is currently the Dean of the School of Engineering and the Director of the Energy, Environment and Climate Change Institute, Hellenic Mediterranean University, Greece. He is/was the scientific coordinator of many European and national funded projects and several private funded projects. His research interests include energy policy, power systems operation, diverse and dispersed generation, micro-grids, renewable energy sources, and energy trading.

• • •